AMERICAN SOCIETY FOR MICROBIOLOGY | Journal of Virology®

Mutation of the Second Sialic Acid-Binding Site, Resulting in Reduced Neuraminidase Activity, Preceded the Emergence of H7N9 Influenza A Virus

Meiling Dai,[a] Ryan McBride,[b] Jos C. F. M. Dortmans,[a]* Wenjie Peng,[b] Mark J. G. Bakkers,[a]* Raoul J. de Groot,[a] Frank J. M. van Kuppeveld,[a] James C. Paulson,[b] Erik de Vries,[a] Cornelis A. M. de Haan[a]

Virology Division, Department of Infectious Diseases and Immunology, Faculty of Veterinary Medicine, Utrecht University, Utrecht, the Netherlands[a]; Departments of Cell and Molecular Biology, Chemical Physiology, and Immunology and Microbial Science, Scripps Research Institute, La Jolla, California, USA[b]

ABSTRACT The emergence of the novel influenza A virus (IAV) H7N9 since 2013 has caused concerns about the ability of the virus to spread between humans. Analysis of the receptor-binding properties of the H7 protein of a human isolate revealed modestly increased binding to α2,6 sialosides and reduced, but still dominant, binding to α2,3-linked sialic acids (SIAs) compared to a closely related avian H7N9 virus from 2008. Here, we show that the corresponding N9 neuraminidases (NAs) display equal enzymatic activities on a soluble monovalent substrate and similar substrate specificities on a glycan array. In contrast, solid-phase activity and binding assays demonstrated reduced specific activity and decreased binding of the novel N9 protein. Mutational analysis showed that these differences resulted from substitution T401A in the 2nd SIA-binding site, indicating that substrate binding via this site enhances NA catalytic activity. Substitution T401A in the novel N9 protein appears to functionally mimic the substitutions that are found in the 2nd SIA-binding site of NA proteins of avian-derived IAVs that became human pandemic viruses. Our phylogenetic analyses show that substitution T401A occurred prior to substitutions in hemagglutinin (HA), causing the altered receptor-binding properties mentioned above. Hence, in contrast to the widespread assumption that such changes in NA are obtained only after acquisition of functional changes in HA, our data indicate that mutations in the 2nd SIA-binding site may have enabled and even driven the acquisition of altered HA receptor-binding properties and may have contributed to the spread of the novel H7N9 viruses.

IMPORTANCE Novel H7N9 IAVs continue to cause human infections and pose an ongoing public health threat. Here, we show that their N9 proteins display reduced binding to and lower enzymatic activity against multivalent substrates, resulting from mutation of the 2nd sialic acid-binding site. This mutation preceded and may have driven the selection of substitutions in H7 that modify H7 receptor-binding properties. Of note, all animal IAVs that managed to cross the host species barrier and became human viruses carry mutated 2nd sialic acid-binding sites. Screening of animal IAVs to monitor their potential to cross the host species barrier should therefore focus not only on the HA protein, but also on the functional properties of NA.

KEYWORDS H7N9, hemagglutinin, influenza A virus, neuraminidase, sialic acid

Influenza A viruses (IAVs) cause seasonal epidemics and occasional pandemics of influenza and therefore pose a significant threat to public health and the economy worldwide. Pandemics are caused by animal IAVs that managed to cross the host

Received 10 January 2017 **Accepted** 4 February 2017

Accepted manuscript posted online 15 February 2017

Citation Dai M, McBride R, Dortmans JCFM, Peng W, Bakkers MJG, de Groot RJ, van Kuppeveld FJM, Paulson JC, de Vries E, de Haan CAM. 2017. Mutation of the second sialic acid-binding site, resulting in reduced neuraminidase activity, preceded the emergence of H7N9 influenza A virus. J Virol 91:e00049-17. https://doi.org/10.1128/JVI.00049-17.

Editor Stanley Perlman, University of Iowa

Address correspondence to Cornelis A. M. de Haan, c.a.m.dehaan@uu.nl.

* Present address: Jos C. F. M. Dortmans, GD Animal Health, Deventer, the Netherlands; Mark J. G. Bakkers, Department of Microbiology and Immunobiology, Harvard Medical School, Boston, Massachusetts, USA.

species barrier and gained the ability to transmit among humans (1). Since 2013, human infections caused by avian-origin H7N9 IAVs have frequently been reported in China, raising concerns about the pandemic threat of these viruses. Although sustained human-to-human transmission has not yet been reported, the novel H7N9 viruses acquired amino acid changes associated with adaptation to human receptor binding and transmission in prior pandemics (2, 3) and appear to transmit from birds to humans more readily than other avian IAVs. In addition, human infections with H7N9 IAVs have a high mortality rate (up to 35%), in part because protective antibodies against the viruses are lacking in humans (4, 5).

IAVs are enveloped, negative-strand RNA viruses that contain two main surface glycoproteins, hemagglutinin (HA) and neuraminidase (NA) (6). HA binds to sialic acid (SIA)-containing receptors on the host cell and triggers fusion of the viral envelope with the endosomal membrane. The NA protein has receptor-destroying activity and, by cleavage of SIAs from glycans, contributes to the release of (progeny) viruses from the host cell surface, as well as from nonfunctional decoy receptors (7, 8). Based on antigenic and genetic properties of these two surface glycoproteins, IAVs are divided into different subtypes. So far, 16 HA (H1 to H16) and 9 NA (N1 to N9) subtypes have been found in wild aquatic birds, which are regarded as the natural reservoir of IAVs (9).

The receptor-binding specificity of the HA protein is a major determinant of IAV host range. While avian IAVs generally prefer binding to α2,3-linked sialosides, human viruses preferentially bind to glycans containing α2,6-linked SIAs (10). Analysis of the receptor-binding properties of the novel H7N9 viruses indicated a dual receptor specificity when complete viruses were used (2, 5, 11, 12). The use of recombinant soluble HA proteins indicated that the novel H7 protein prefers binding to avian-type receptors (α2,3-linked sialosides) while also displaying weak binding to human-type receptors (α2,6-linked sialosides) (2, 13–15). Binding to avian-type receptors was reduced, however, in comparison to ancestral avian H7 viruses (15). Mutational analysis showed that substitutions at positions 186 and 226 were largely responsible for the observed altered receptor-binding properties of the novel H7 protein (15).

The balance between the HA and NA activities is considered critical for IAV replication and transmissibility. Changes in the receptor-binding properties of the HA protein are often accompanied by changes in the enzymatic properties of NA (16, 17). The type II transmembrane NA protein forms a homotetramer with each NA monomer, consisting of a globular head domain, a thin stalk of variable length, a hydrophobic transmembrane domain (TMD), and a short N-terminal cytoplasmic tail. The NA head domain contains the active site, composed of highly conserved catalytic and structural residues that either directly contact the SIA or stabilize the catalytic residues (6, 18, 19). In contrast to the detailed knowledge on the receptor-binding specificity of the HA protein, little is known about the cleavage specificity of the NA protein compared to the receptor-binding properties of the HA protein. In general, it seems that NA proteins from both avian and human viruses prefer cleavage of α2,3 over α2,6 SIAs, although this difference appears smaller for the NA of human IAVs (20–22). However, in most studies, cleavage of only a very limited number of synthetic glycans was analyzed.

The NA proteins of several avian IAVs (N1, N2, and N9) have been shown to display hemadsorption activity (23–26), which was attributed to the presence of a 2nd SIA-binding site. For N9, X-ray crystallography (27) revealed that the 2nd SIA-binding site is a shallow pocket composed of three surface peptide loops, located adjacent to the catalytic site. The presence of a 2nd SIA-binding site in N1 was also demonstrated using saturation transfer difference (STD) nuclear magnetic resonance (NMR) spectroscopy (28). By both hemadsorption assays and STD NMR, it was shown that N1 and N2 proteins of swine and human IAVs display severely reduced binding compared to their avian counterparts (26, 28). Sequence analysis indicated that five out of six SIA contact residues in the N9 2nd SIA-binding site are highly conserved across all avian NA genotypes. This conservation is lost in human N1 and N2 genotypes, in agreement with the $>$100-fold-reduced hemadsorption activity reported for their NAs (17, 26, 29). The biological significance of the 2nd SIA-binding site in avian NAs remains elusive, and

essentially nothing is known about its SIA-binding specificity. It has been suggested that the site may serve to enhance the catalytic efficiency of NA, as changes in hemadsorption activity of N2 were correlated with changes in the ability of N2 to cleave SIA from multivalent, but not monovalent, substrates (26).

Previously, we compared the HA receptor-binding properties of a human isolate of the novel H7N9 virus isolated in 2013 with those of a closely related avian H7N9 virus from 2008. In line with the results obtained by others (13, 14), the H7 of the novel H7N9 virus displayed modestly increased binding to α2,6 sialosides and reduced, but still dominant, binding to α2,3-linked SIAs compared to the H7N9 virus from 2008 (15). In the present study, we analyzed the enzymatic activities and binding properties of the corresponding N9 proteins of these H7N9 viruses. After optimizing the recombinant protein expression approach for NA, we analyzed the enzymatic activities of the N9 proteins using monovalent and multivalent substrates. The results indicate that the two N9 proteins display equal specific activities on the monovalent substrate 2′-(4-methylumbelliferyl)-α-D-*N*-acetylneuraminic acid (MUNANA) and similar substrate specificities, as revealed by glycan array analysis. In addition, glycan array analysis was for the first time used to determine the binding specificity of the 2nd SIA-binding site. Binding and substrate specificity, as revealed by glycan array analyses, were shown to correlate well for the avian N9 protein from 2008. The novel N9 protein displayed reduced binding to and enzymatic activity against multivalent substrates. Mutational analysis, involving loss- and gain-of-function NA phenotypes, attributed these differences to a T401A substitution in the 2nd SIA-binding site. Phylogenetic analysis indicated this substitution was unique to the novel H7N9 viruses. Remarkably, the T401A mutation in NA preceded the mutations found in H7 at positions 186 and 226, which are essential for the altered receptor-binding properties of the virus, indicating that mutations in the 2nd SIA-binding site may have enabled the acquisition of altered receptor-binding properties of HA.

RESULTS

Comparison of enzymatic activities of different recombinant soluble N9 constructs. Previously, we compared the HA receptor-binding properties of a novel H7N9 virus isolated from a human patient in 2013 (A/Anhui/1/2013, referred to as "Anhui") with those of a closely related avian H7N9 virus from 2008 (A/Anas crecca/Spain/1460/2008, referred to as "Spain") (15). In the same study, we also made a preliminary comparison of the enzymatic properties of the corresponding N9 proteins. Detailed analysis of the N9 proteins was precluded, however, by the low expression levels and activities of the recombinant soluble N9 proteins. These proteins consisted of the NA head domain (residues 76 to 469 of the N9 protein) N-terminally extended with a GCN4-pLI tetramerization domain (15) (referred to in this study as GCN4-N9$_{head}$) (Fig. 1A). However, the NA stalk domain may contribute to correct folding (30) and affect enzymatic activity (31, 32). Therefore, we constructed novel expression vectors encoding N9 protein head domains extended with their stalk sequences (Fig. 1A) (starting with residue 42, referred to as GCN4-N9). The GCN4-N9 proteins migrated, as expected, at a higher position in the gel than the GCN4-N9$_{head}$ proteins lacking the stalk domain (Fig. 1B) and displayed 2- to 3-fold higher expression levels. Importantly, in the MUNANA assay, the GCN4-N9 proteins displayed much higher specific activity than the GCN4-N9$_{head}$ proteins (Fig. 1C). We previously showed that replacing GCN4-pLI with a tetrabrachion tetramerization domain also resulted in NA proteins with higher specific activity (31), and therefore, we made N9 constructs with such a tetrabrachion domain. The resulting proteins (referred to as TE-N9) displayed the expected electrophoretic mobility (Fig. 1B) and higher specific activity than the GCN4-N9 proteins (Fig. 1C). Specific activities for MUNANA were similar for the N9 Anhui and Spain proteins. TE-N9 proteins displaying the highest specific activity were used in all subsequent analyses.

Enzymatic activity of the TE-NA N9 proteins with multivalent substrates. Next, we analyzed the enzymatic activities of the TE-N9 Anhui and Spain proteins on multivalent, surface-coated fetuin and transferrin glycoprotein substrates, which

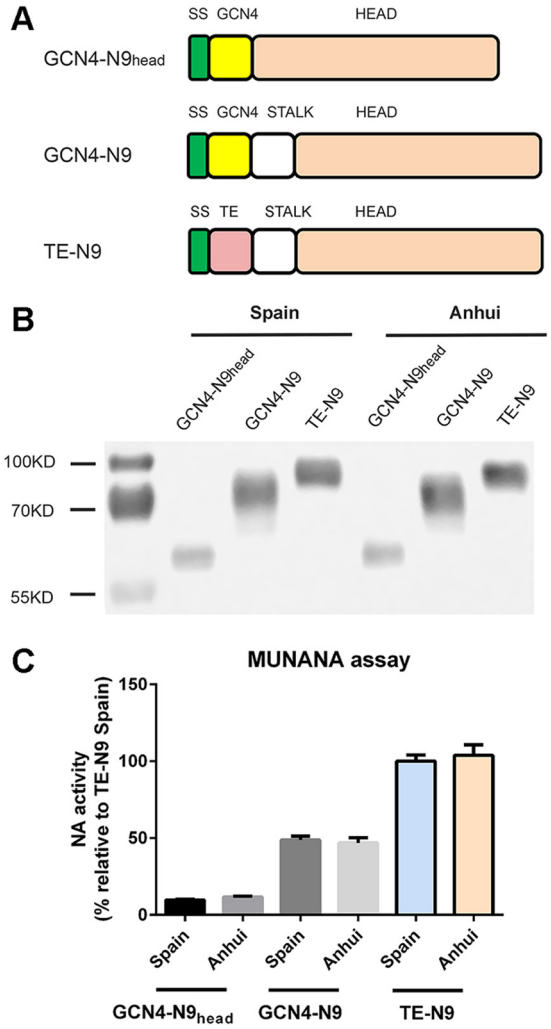

FIG 1 Optimization of the recombinant soluble N9 expression approach. (A) Schematic representation of the recombinant soluble N9 proteins. GCN4-$N9_{head}$ contains the NA head, the GCN4 tetramerization domain (GCN4), and a cleavable signal sequence (SS). The GCN4-N9 construct contains the head and stalk regions fused with GCN4 and a signal sequence. TE-N9 proteins have a schematic structure similar to that of GCN4-N9 but carry a tetrabrachion (TE) instead of the GCN4 domain. (B) Expression of the different versions of the N9 Spain and Anhui proteins in HEK293T cells was analyzed by SDS-PAGE, followed by Western blotting. The positions on the gel of the relevant molecular mass marker proteins are shown. (C) Specific activities of the different N9 Spain and Anhui proteins using the MUNANA substrate normalized to that of TE-N9 Spain. The means of the results of three independent experiments performed in triplicate are graphed. The error bars indicate standard deviations.

better resemble the multivalent *in vivo* substrates of NA than the soluble monovalent MUNANA substrate. Fetuin contains mono-, bi-, and triantennary glycans with α2,3- and α2,6-linked SIAs in a 2:1 ratio (33). Transferrin contains two biantennary N-linked glycan chains with only α2,6-linked SIAs (34, 35), which was confirmed (data not shown) by linkage-type-specific enzyme-linked lectin-binding assays (ELLA). Fetuin- and transferrin-coated 96-well plates were incubated with serially diluted TE-NA proteins, after which the resulting cleavage of SIAs was quantified by probing the 96-well plates with lectins with different binding specificities. *Erythrina crista-galli* lectin (ECA) specifically recognizes glycans containing terminal Galβ1-4GlcNAc, which generally correspond to desialylated N-linked sugars (36), while peanut agglutinin (PNA) binds to terminal Galβ1-3GalNAc, corresponding to desialylated O-linked sugars (37). *Maackia amurensis* lectin I (MAL I) and *Sambucus nigra* lectin (SNA) specifically bind α2,3- or α2,6-linked SIAs, respectively (38, 39). From the resulting curves, the specific activities (activity per amount of protein) of the TE-N9 proteins were determined for each

glycoprotein-lectin combination, as indicated in Materials and Methods, and plotted relative to the specific activity determined for fetuin-ECA. Both TE-N9 proteins displayed higher specific activity when fetuin was used as a substrate than with transferrin (Fig. 2A and B). This substrate preference corresponds to both proteins preferring cleavage of α2,3-linked (determined with fetuin-MAL I) over α2,6-linked (determined with fetuin-SNA and transferrin-SNA) SIAs (Fig. 2A and B). Potential fine specificity was investigated in detail by assessing cleavage of SIA from a large number of sialylated glycans on a glycan array. Cleavage of SIAs was quantified by binding of fluorescently labeled ECA. The results (Fig. 2C and D; see Table S1 in the supplemental material) indicated that both TE-N9 proteins prefer cleavage of α2,3- over α2,6-linked sialosides. Bi- and triantennary glycans containing multiple LacNAc repeats were most efficiently cleaved, although this observation may partly reflect the high affinity of ECA for such glycans (36). The TE-N9 Anhui protein was less active than the TE-N9 Spain protein in the glycan array analysis. Direct comparison of the specific activities on fetuin and transferrin revealed that the TE-N9 Spain protein indeed had higher specific activity than the TE-N9 Anhui protein (Fig. 2E and F). In summary, we conclude that the N9 Spain and Anhui proteins display similar cleavage specificities. Furthermore, although the two proteins do not differ in their specific activities when using a monovalent soluble MUNANA substrate, the N9 Spain protein has a higher specific activity than the N9 Anhui protein when substrates are presented in a multivalent manner.

Binding of N9 proteins to sialosides. Mutations in the 2nd SIA-binding site of N2, which resulted in severely reduced hemadsorption activity, were previously shown to affect the catalytic efficiency of NA against multivalent, but not monovalent, substrates (26). Differences in specific activities for multivalent substrates of the two N9 proteins (which have similar specific activities for monovalent MUNANA) may therefore be caused by differences in their abilities to bind to multivalent substrates. To test this hypothesis, the TE-N9 proteins were subjected to different glycoprotein binding assays, similar to what has been performed previously for different HA proteins (15, 40). The results show that the TE-N9 proteins indeed differ in their abilities to bind fetuin, with the Spain and Anhui proteins displaying efficient and negligible binding, respectively (Fig. 3A and B) in the presence of the NA inhibitor oseltamivir carboxylate (OsC). OsC occupies the NA active site, inhibits NA activity, and prevents binding of substrates via the active site. No binding was observed without OsC or when desialylated fetuin was used (data not shown). As positive controls, the H7 Spain and Anhui proteins were taken along with N9 Spain and Anhui proteins for binding assays. In agreement with previous results (15), the H7 Anhui protein bound fetuin with lower avidity than the H7 Spain protein. Similar differences between the H7 and N9 proteins were observed in a hemagglutination assay (Fig. 3C). The binding specificities of the N9 proteins were studied in more detail using glycan array analysis. The N9 Spain protein displayed efficient binding to a large number of α2,3-linked sialosides and weak or no binding to α2,6-linked sialosides. Glycan structures lacking SIAs did not bind (Fig. 4A; see Table S1 in the supplemental material). Glycans that were efficiently bound by N9 were also efficiently cleaved (Fig. 4C). In agreement with the fetuin-binding and hemagglutination assay, little binding, if any, was observed for the N9 Anhui protein (Fig. 4B; see Table S1 in the supplemental material).

Sequence and structural analysis of N9 proteins. Protein sequence alignment showed that the Anhui and Spain N9 proteins differ at only 8 amino acid positions, in addition to a small deletion of 5 amino acids in the stalk (Fig. 5A). None of these changes were located in or directly adjacent to the enzyme active site in the three-dimensional (3D) structure (Fig. 5B). However, Thr401 (N2 numbering) is part of a loop (residues 399 to 403, shown in green) that forms an H bond via Asn400 with SIA bound to the 2nd SIA-binding site (Fig. 5B to D) and provides a crucial stacking interaction between the SIA 5-*N*-methyl group and the aromatic side chain of Trp403. Thr401 is not in direct contact with the bound SIA, but replacement of Thr401 by Ala401 in N9 Anhui results in loss of a water-mediated hydrogen bond to Asp402. Loss of this interaction

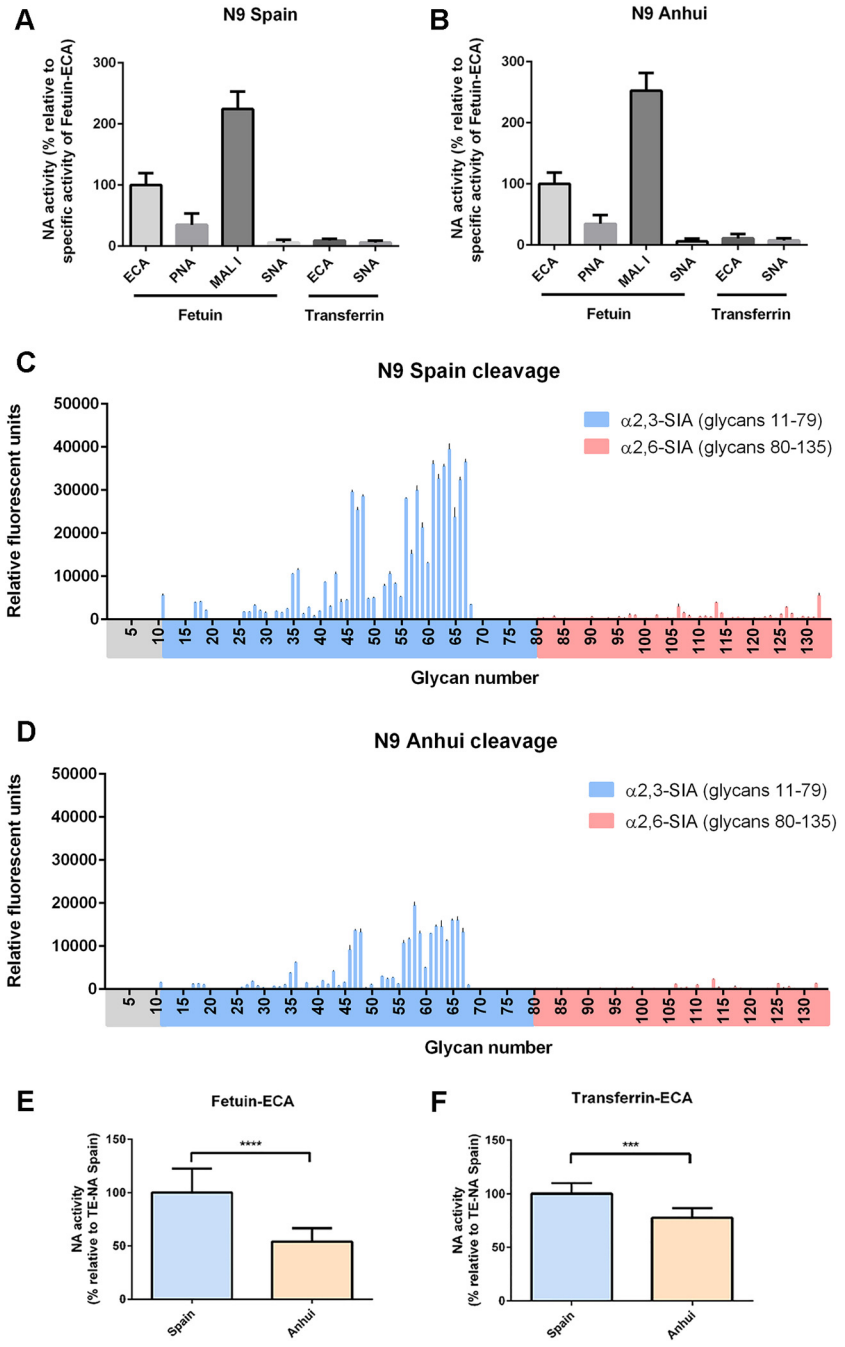

FIG 2 Specific activities and cleavage specificities of the N9 proteins. (A) Specific activity of TE-N9 Spain as determined by ELLA using different glycoprotein-lectin combinations normalized to that of fetuin-ECA. (B) Specific activity of TE-N9 Anhui as determined by ELLA using different glycoprotein-lectin combinations normalized to that of fetuin-ECA. (C and D) Glycan array analysis of the cleavage specificities of N9 Spain (C) and Anhui (D). Desialylation of the glycans was detected by ECA binding. The colors of the bars correspond to the types of SIA. The numbers correspond to the numbers in Table S1 in the supplemental material. Glycans that were bound by ECA without NA treatment were excluded from the analysis (nonsialylated glycans 1 to 10). Desialylated glycan structures that cannot be bound by ECA were also excluded from the analysis; upon desialylation, these glycans contain terminal Galβ1-3GlcNAc (glycans 15, 21 to 23, and 51), Galβ1-3GalNAc (glycans 24, 25, and 31), Galβ1-4Glc (glycans 16, 70, 71, and 82), GalNAcβ1-4Gal (glycans 20 and 86), 6S-Galβ1-4GlcNAc (glycans 13 and 14), or Galβ1-4GlcNAc with GlcNAc fucosylated (glycans 12, 14, and 72 to 79). The glycan array values shown are the means and standard errors of 6 glycan spot intensities, while the error bars indicate standard errors of the mean (SEM). (E and F) Specific activities of TE-N9 Spain and Anhui as determined by ELLA using fetuin (E) or transferrin (F) in combination with ECA normalized to that of TE-N9 Spain. The means of the results of three or four independent experiments performed in duplicate/triplicate are shown for the ELLA. Standard deviations are indicated. Significant differences were determined using the Student *t* test: ***, $P < 0.001$; ****, $P < 0.0001$.

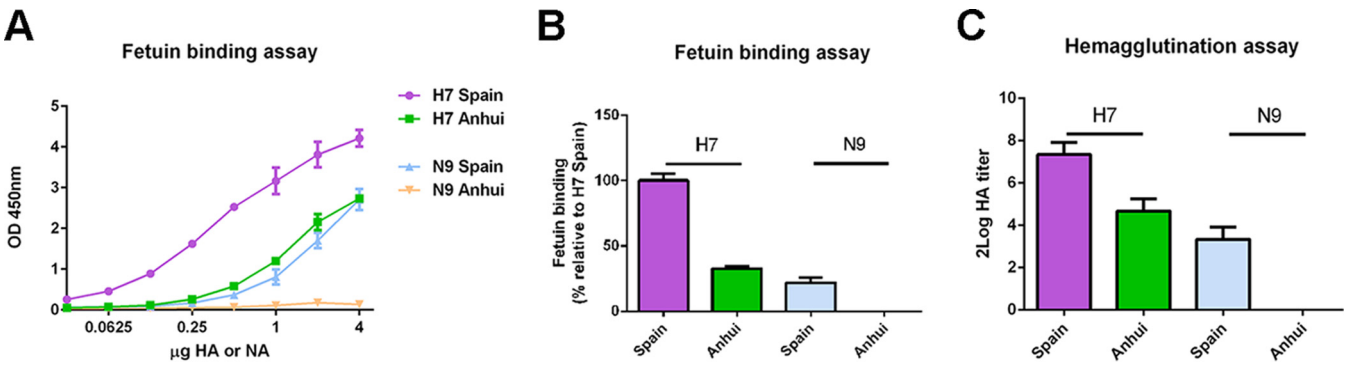

FIG 3 Binding properties of recombinant soluble N9 proteins. (A) Limiting dilutions of soluble H7 or N9 proteins complexed with HRP-conjugated antibodies were applied in a fetuin-binding assay; 1 μM OsC was added to the NA samples to inhibit NA catalytic activity. The optical density at 450 nm corresponds to binding of the indicated proteins to fetuin. The results of a representative experiment are shown. (B) Curves, similar to those shown in panel A, of the results of three independent experiments were used to determine the amount of HA or NA protein corresponding to half-maximum binding. The inverse of this amount is a measure of the relative binding avidity and was normalized to that of H7 Spain. (C) Hemagglutination titers of antibody-complexed recombinant soluble H7 and N9 proteins. The means of the results of three independent experiments performed in duplicate are shown. Standard deviations are indicated.

may increase the flexibility and possibly affect local folding of the 2nd SIA-binding site and thereby reduce binding to SIA.

The residue at position 401 is largely responsible for the different N9 properties. To determine whether Thr401 in the 2nd SIA-binding site is important for binding to and cleavage of multivalent substrates, the T401A and the A401T mutations were introduced into the Spain and Anhui N9 proteins, respectively. The wild-type and mutant proteins were subsequently subjected to different binding assays. Mutation of the residue at position 401 either abolished (Spain-T401A) or established (Anhui-A401T) binding of the N9 proteins to fetuin (Fig. 6A) and to red blood cells (Fig. 6B). Similarly, the T401A substitution in the Spain N9 protein decreased binding, as determined by glycan array analysis, while the reciprocal effect was observed for the A401T mutation in the Anhui protein (Fig. 6C and D; see Table S1 in the supplemental material). Next, we analyzed the enzymatic activities of the mutant N9 proteins. Mutation of the residue at position 401 had no effect on the specific activity using the monovalent MUNANA substrate (Fig. 6E), nor did it change the cleavage specificity (see Table S1 in the supplemental material). This is in agreement with the Anhui and Spain proteins displaying similar substrate specificities and specific activities using MUNANA. However, in agreement with the binding assay results, the introduction of substitution T401A in the Spain N9 protein decreased the specific activity when using the multivalent fetuin substrate. The reciprocal effect was observed after introduction of the A401T substitution in the Anhui protein (Fig. 6F to H). Thus, the ability of N9 proteins to cleave SIAs from fetuin corresponds to their binding avidities to the glycoprotein. These differences could be largely attributed to the residue at position 401 in the 2nd SIA-binding site.

Phylogenetic analysis of N9 proteins. To get more insight into the evolutionary history of the N9 and H7 proteins of the novel H7N9 viruses, phylogenetic analyses were performed (Fig. 7 and 8 and Table 1). The results indicate that the T401A mutation in N9 is unique to the novel H7N9 viruses and occurs at the root of the novel H7N9 clade, after which it is strictly conserved (Fig. 7). The T401A mutation preceded a small, 5-amino-acid deletion in the stalk, which has been described previously as being characteristic of the novel H7N9 viruses (41) (Table 1). The phylogenetic analyses, furthermore, indicate that only after the acquisition of these NA mutations are the substitutions in H7 at positions 186 and 226, which are associated with the altered receptor-binding properties of these viruses (15), observed (Fig. 8 and Table 1).

DISCUSSION

Compared to its well-studied functional counterpart HA, much less is known about the binding and cleavage properties of the IAV NA protein. In the present study, the detailed binding properties of the 2nd SIA-binding site of IAV NA were analyzed in

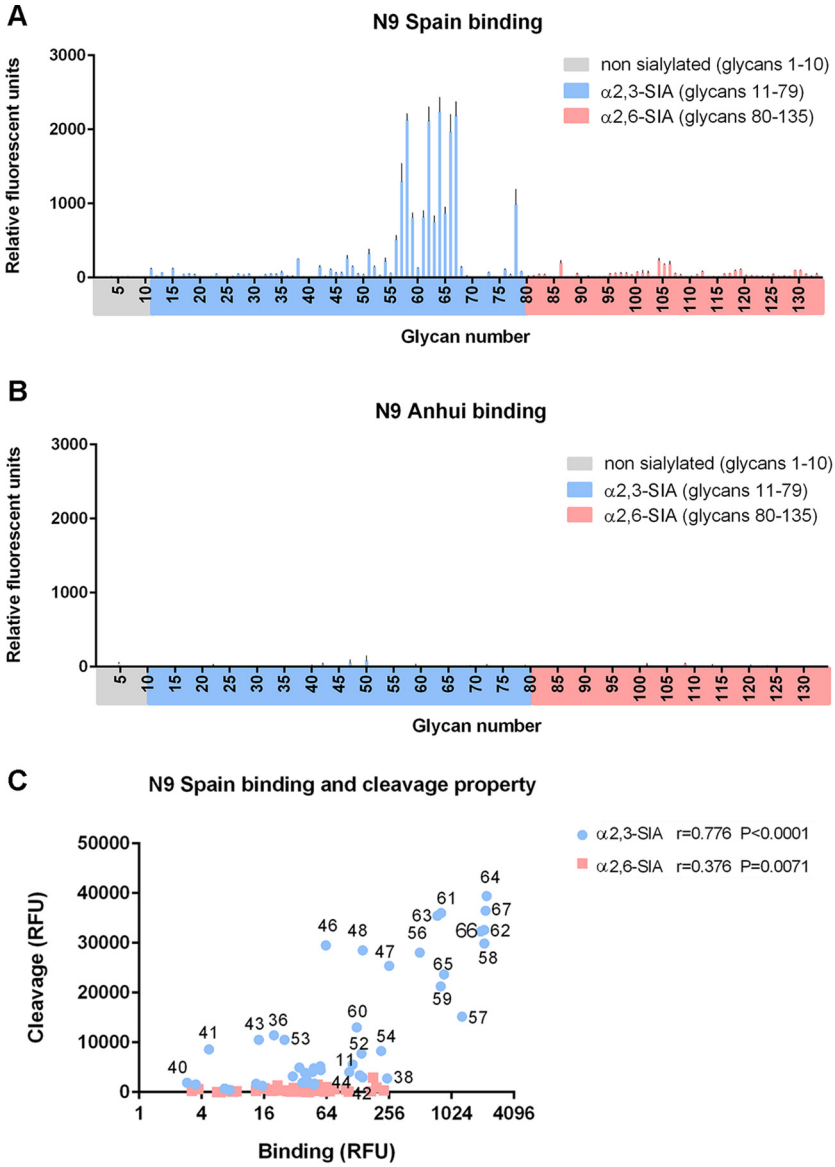

FIG 4 N9 binding specificity determined by glycan array assay. (A and B) Glycan array analysis of the binding specificities of N9 Spain (A) and Anhui (B) in the presence of 1 μM OsC. In addition, binding to nonsialylated glycans was evaluated (glycans 1 to 10). The glycan array values shown are the means and standard errors of 6 glycan spot intensities, the error bars indicate SEM. (C) Scatterplot of binding to and cleavage of glycans on the array by N9 Spain. Pearson correlation coefficients (*r*) and the corresponding *P* values are indicated for each of the sialoside types. The numbers correspond to those in Table S1 in the supplemental material. RFU, relative fluorescent units.

correlation with NA cleavage properties for the first time, using glycan array analyses. Our study establishes the functional significance of the 2nd SIA-binding site, which has long remained underappreciated. Analysis of N9 proteins of the novel H7N9 IAVs that have been infecting humans since 2013 allowed us to directly correlate NA cleavage with NA binding via the 2nd SIA-binding site. Substrate binding via this site clearly enhances NA catalytic efficiency against the same substrate. A single T401A mutation in the NA 2nd SIA-binding site of novel H7N9 viruses, which reduced binding to and cleavage of multivalent substrates, appears to functionally mimic the substitutions that are found in the 2nd SIA-binding site of NA proteins of IAVs that managed to cross the host species barrier to become human viruses (20, 26, 42). However, in contrast to the widespread assumption that such changes in NA are obtained only after acquisition of functional changes in HA, our phylogenetic analyses indicated that the T401A substi-

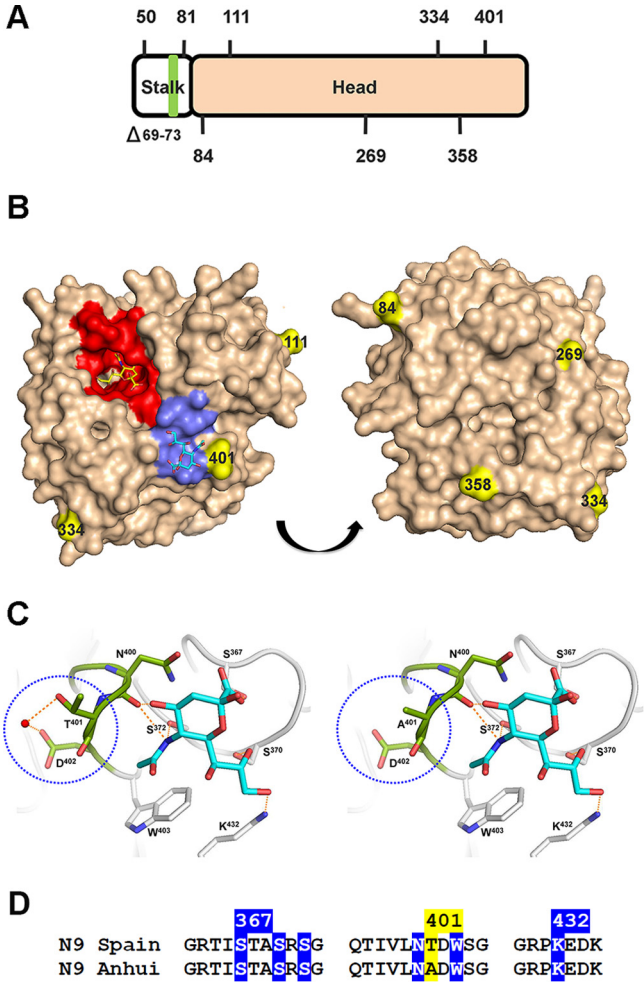

FIG 5 Sequence and structural analysis of the N9 proteins. (A) Schematic representation of the residues that differ between the recombinant soluble N9 Spain and Anhui proteins. Two residues are located in the NA stalk domain, while another 6 residues are located in the NA head domain. The 5-amino-acid NA stalk deletion observed in N9 Anhui is indicated by the green rectangle. (B) Crystal structure of N9 from A/tern/Australia/G70C/75 in complex with Neu5Ac (Protein Data Bank [PDB] accession no. 1MWE) (27) depicted using PyMol software. Top and bottom views are shown. The NA active site (6) and the residues in the 2nd SIA-binding site that have direct interaction with SIA (27) are colored red and blue, respectively. The Neu5Ac moieties in these sites are shown as sticks. Residues that differ between N9 Spain and Anhui in the NA head region are colored yellow. The residues that differ in the stalk region are not indicated, as the structure of this part of NA is not solved. (C) Crystal structure of the secondary receptor-binding site of NA in complex with Neu5Ac (PDB accession no. 1MWE). NA and Neu5Ac are shown as sticks (oxygen in red, nitrogen in blue, and carbon in gray or green [for NA] or cyan [for Neu5Ac]), and water molecules are shown as red spheres and hydrogen bonds as dashed orange lines. The image was made using PyMOL. (D) Sequence alignment of the three loops that form the 2nd SIA-binding site and surrounding residues of the Anhui and Spain N9 proteins. Residues in the 2nd SIA-binding site that have direct interaction with SIA are shaded in blue. The residue at position 401 that differs between the Spain and Anhui N9 proteins is shaded in yellow. The N2 numbering of some residues is indicated.

tution in N9 occurred prior to substitutions in HA causing the altered receptor-binding properties of novel H7N9 viruses. Possibly, the initial functional changes in the N9 protein have subsequently enabled the acquisition of altered receptor-binding properties of the H7 protein and may contribute, in addition to the mutations found in HA, to the spread and the increased ability of the virus to infect humans in comparison to other avian viruses.

The presence of a 2nd SIA-binding site in NA was already demonstrated in the 1980s using hemadsorption assays (23–25). Direct experimental evidence for the presence of this site was obtained decades later by X-ray crystallography (27) and STD NMR (28), but

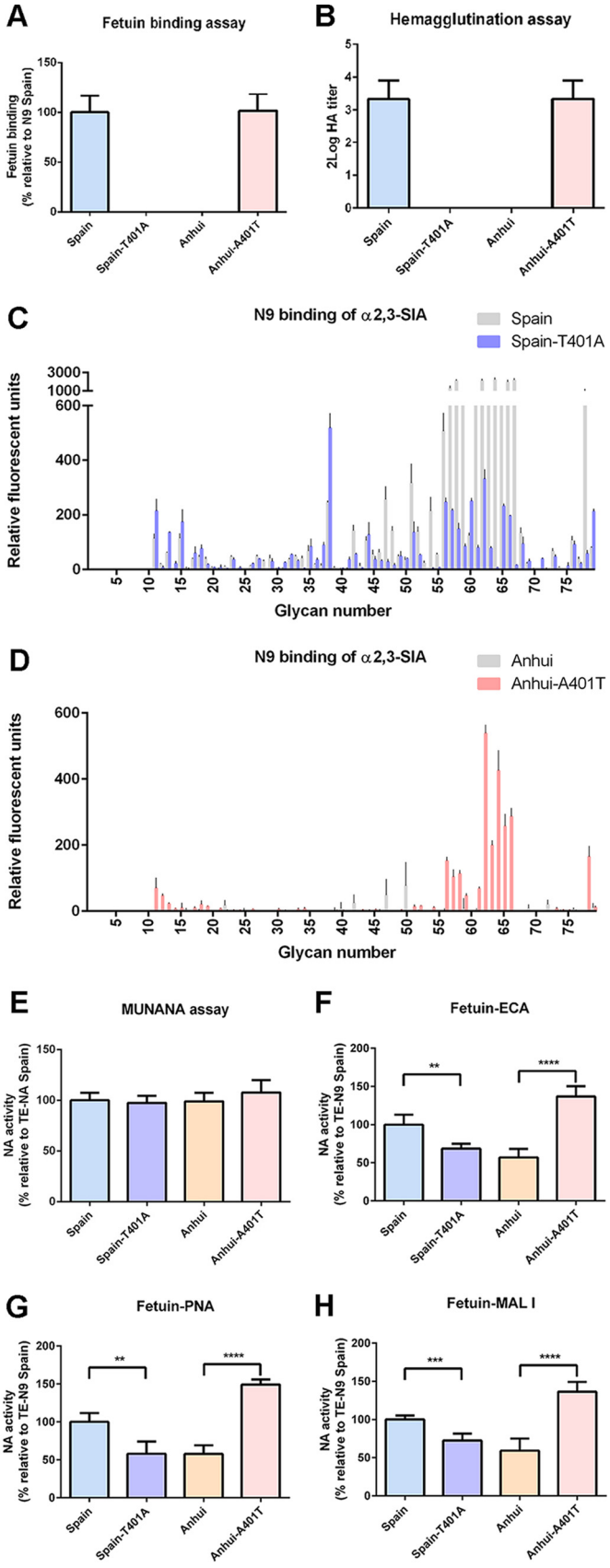

FIG 6 Effects of substitutions at position 401 on N9 binding and enzymatic activity. (A to D) Binding properties of wild-type N9 proteins, as well as their counterparts with substitutions at position 401,

(Continued on next page)

detailed analysis of its binding specificity was lacking. By using glycan array analysis, we now show that the N9 protein of an avian IAV prefers binding to α2,3-linked sialosides, particularly the bi- and triantennary glycans with multiple LacNAc repeats. No binding was observed to α2,6-linked sialosides. In contrast, the 2nd SIA-binding site of a cell surface-expressed N2 protein was shown to enable binding to red blood cells that had been resialylated using either α2,3 or α2,6 sialyltransferases with approximately equal efficiency (26). Whether this difference reflects different binding specificities for the N2 and N9 proteins or resulted from the different experimental setups remains to be determined.

The biological function of the NA 2nd SIA-binding site has long remained elusive. Only a single study showed that the ability of NA to bind red blood cells corresponded to the cleavage efficiencies of other multivalent substrates (26). We now directly show that substrate binding via the 2nd SIA-binding site enhances NA catalytic efficiency against the same substrate. The 2nd SIA-binding site, which is adjacent to the actual NA active site, may enhance the catalytic efficiency of NA by recruiting and keeping multivalent sialosides close to the active site (26, 43). Enhancement of catalytic efficiency resulting from catalytic and carbohydrate-binding domains interacting simultaneously with a polyvalent substrate appears to be a general feature of most glycoside hydrolases, as most of these enzymes have been shown to contain lectin domains, including eukaryotic and bacterial NA proteins (44), as well as other viral-receptor-destroying enzymes (45, 46).

The presence of a 2nd SIA-binding site provides IAV with an additional, potentially more subtle option to modulate the catalytic efficacy of its NA protein by circumventing the necessity for mutation of the highly conserved key residues in the NA catalytic site. This mechanism may allow IAV to readily achieve an optimal HA-NA balance when adapting to a novel receptor repertoire upon infection of a novel host species and/or when coping with HAs with altered receptor-binding properties. For example, the emergence of pandemic human IAVs was accompanied not only by the well-known changes in the receptor-binding properties of the HA proteins, but also by changes in the NA 2nd SIA-binding site, which decrease hemadsorption activity (17). We now show that modulation of the NA catalytic activity via mutation of the 2nd SIA-binding site may also be observed for avian IAVs. The decreased ability of the N9 protein of novel H7N9 IAV to bind and cleave sialosides correlates well with the low receptor-binding avidity of the corresponding HA protein (15). Moreover, the substitution at position 401 shows that substrate binding via the 2nd SIA-binding site may be modulated by mutation of residues in the 2nd SIA-binding site other than those that directly contact the SIA moiety. It will be of interest to study the effects of other substitutions in NA proteins of avian viruses at positions neighboring the highly conserved SIA contact residues in the 2nd SIA-binding site.

Decreased receptor binding of the N9 protein of the novel H7N9 viruses is another property in which the virus appears to resemble (early) human viruses, besides its decreased and modestly increased HA binding to avian- and human-type receptors, respectively. However, in contrast to the widespread assumption that such changes in NA are obtained only after acquisition of functional changes in HA, our phylogenetic analyses indicate that the T401A substitution in the 2nd SIA-binding site was obtained

FIG 6 Legend (Continued)
determined by fetuin-binding (A), hemagglutination (B), and glycan array (C and D) assays in the presence of 1 μM OsC similarly to what was described in the legends to Fig. 3 and 4. Only binding to nonsialylated (glycans 1 to 10) and α2,3-SIA (glycans11 to 79) glycans is shown. The glycan array values shown are the means and standard errors of 6 glycan spot intensities. (E to H) Specific activities of N9 and mutant proteins determined by MUNANA assay (E) or by ELLA using fetuin in combination with different lectins (ECA [F], PNA [G], and MAL I [H]) normalized to that of N9 Spain. The means of the results of three or four independent experiments performed in duplicate/triplicate are shown for the fetuin-binding and hemagglutination assays and ELLA. Standard deviations are indicated. Significant differences between wild-type proteins and their mutants as determined by Student *t* test are indicated: **, $P < 0.01$; ***, $P < 0.001$; ****, $P < 0.0001$.

FIG 7 Phylogenetic analysis of N9 proteins derived from HxN9 and novel H7N9 viruses. An N9 protein tree was constructed as described in Materials and Methods. Key residues that differ between different branches are indicated. The N9 protein tree is rooted by the A/Anas crecca/Spain/1460/2008 isolate (N9 Spain). The two N9 proteins (N9 Anhui and Spain) that were compared in the present study are boxed in red. The mutation at position 401 and the deletion in the stalk are boxed in green.

prior to the acquisition of mutations in H7 (at position 186 and 226) that are responsible for the altered receptor-binding properties (2, 15). The T401A mutation in NA, possibly in combination with the small stalk deletion, may therefore have allowed and even have driven these altered HA properties to restore the balance between HA and NA. Although it is not clear why and in which animal species these mutations in NA and HA were selected, it seems plausible that they have contributed to the wide spread of the novel H7N9 viruses and to the relatively high ability of these avian viruses to infect humans. In view of our results, genotypic and phenotypic screening of animal IAVs to monitor their potential to cross the host species barrier should focus not only on the

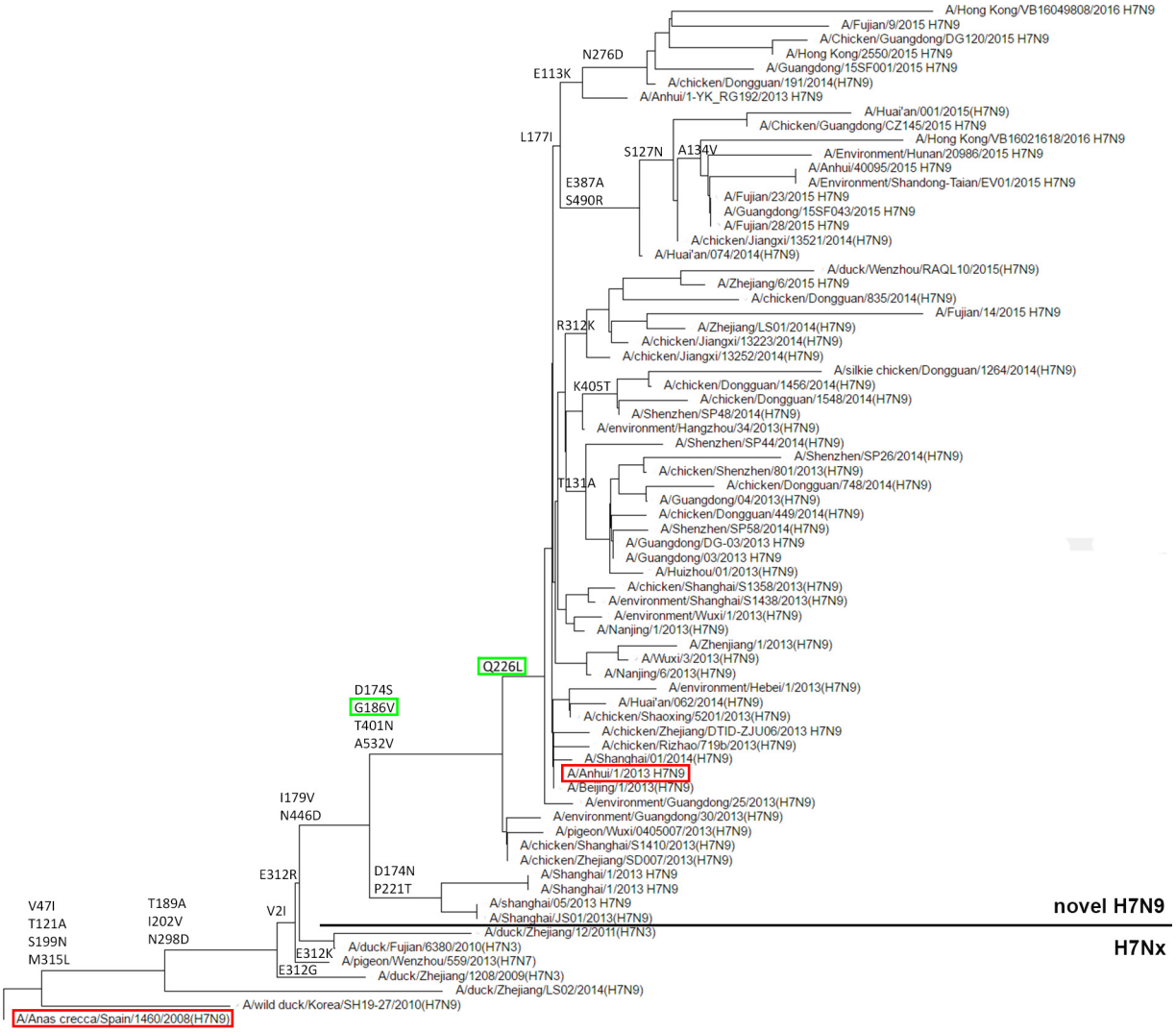

FIG 8 Phylogenetic analysis of HA proteins derived from H7Nx and novel H7N9 viruses. An H7 protein tree was constructed as described in Materials and Methods. Key residues that differ between different branches are indicated. The H7 protein tree is rooted by the A/Anas crecca/Spain/1460/2008 isolate (H7 Spain). The two H7 proteins (H7 Anhui and Spain) corresponding to the N9 proteins that were compared in the present study are boxed in red. The mutations at positions 186 and 226 that are responsible for the altered receptor-binding properties of the H7 Anhui protein are boxed in green.

HA protein, but also on the catalytic properties of NA using the appropriate multivalent substrates.

MATERIALS AND METHODS

Genes, expression vectors, and protein expression and purification. Expression constructs of the recombinant soluble H7 and N9 proteins of A/Anhui/1/2013 (GISAID isolate EPI439507, referred to as H7 Anhui and N9 Anhui) and of A/Anas crecca/Spain/1460/2008 (GenBank accession no. CAY39406 and HQ244409.1, referred to as H7 Spain and N9 Spain) have been described previously (15). In these N9 expression constructs, sequences encoding the NA head domain (amino acids 76 to 470) of N9 Anhui and N9 Spain were preceded by sequences encoding a CD5 N-terminal signal sequence, a double Strep tag for purification (One-STrEP; IBA GmbH), and a GCN4-pLI (47) tetramerization domain (referred to as GCN4-NA_{head}). The NA ectodomain-encoding sequences in the construct were extended with sequences encoding the stalk domain (starting at residue 42) by insertion of a primer dimer and cloned into a pFRT expression plasmid (Thermo Fisher Scientific) downstream of sequences encoding the signal peptide of *Gaussia* luciferase and GCN4-pLI (referred to as GCN4-NA) (31). Finally, the GCN4-pLI tetramerization domain was exchanged with the *Staphylothermus marinus* tetrabrachion tetramerization domain (31, 48) (referred to as TE-NA). Mutations of interest were introduced into the corresponding NA genes by using the Q5 site-directed mutagenesis kit (NEB) and confirmed by sequencing. HA and NA expression plasmids were transfected into HEK293T cells (ATCC), and recombinant soluble NA or HA proteins were purified from the cell culture supernatants using Strep-tactin beads (IBA) as described previously (40).

TABLE 1 Occurrence of key residues in H7 and N9 proteins

	N9 protein		H7 protein	
Influenza A virus	**401**	**Δ69–73[a]**	**186**	**226**
H7Nx and HxN9 prior to 2013[b]	T	−	G	Q
A/Anas crecca/Spain/1460/2008	T	−	G	Q
A/Shanghai/05/2013	A	−	G	Q
A/Shanghai/JS01/2013	A	−	G	Q
A/Shanghai/1/2013	A	+	G	Q
A/Shanghai/1b/2013	A	+	G	Q
A/chicken/Zheijang/SD007/2013	A	+	V	Q
A/chicken/Shanghai/S1410/2013	A	+	V	Q
A/pigeon/Wuxi/0405007/2013	A	+	V	Q
A/environment/Guangdong/30/2013	A	+	V	Q
A/Bejing/1/2013	A	+	V	L
A/Nanjing/1/2013	A	+	V	L
A/environment/Guangdong/25/2013	A	+	V	L
A/Anhui/1/2013	A	+	V	L
A/chicken/Dongguan/748/2014	A	+	V	L
A/Fujian/9/2015	A	+	V	L
A/Hong Kong/VB16021618/2016	A	+	V	L

[a]Δ69–73 indicates a deletion of 5 amino acids in the NA stalk. − and + indicate the absence or presence, respectively, of the deletion.

[b]The only exception is the N9 protein of A/Zheijang/LS02/2012 H11N9, which also contains the 5-amino-acid (Δ69–73) deletion in the NA stalk.

Quantification of the purified proteins was performed by comparative Coomassie gel staining using standard bovine serum albumin (BSA) samples (Sigma-Aldrich) with known concentrations as a reference.

NA enzymatic assays. Purified N9 proteins were assayed for the ability to cleave different substrates. The activity of N9 proteins toward the synthetic monovalent substrate MUNANA (Sigma-Aldrich) was determined by using a fluorometric assay similarly to what was described previously (31) with a Fluostar Optima plate reader (BMG Labtech, Mornington, Australia) with excitation and emission wavelengths at 340 and 490 nm, respectively. The activities of the NA proteins toward multivalent glycoprotein substrates were analyzed using a previously described ELLA (49) with some modifications. In brief, 2.5 μg/ml fetuin-coated or 25 μg/ml transferrin-coated (both from Sigma-Aldrich) 96-well Nunc MaxiSorp plates were incubated with serial dilutions of recombinant soluble NA proteins in reaction buffer (50 mM Tris-HCl, 4 mM $CaCl_2$, pH 6.0). After overnight incubation at 37°C, the plates were washed and incubated with either biotinylated ECA (1.25 μg/ml; Vector Laboratories), biotinylated PNA (2.5 μg/ml; Galab Technologies), biotinylated SNA (1.25 μg/ml; Vector Laboratories), or biotinylated MAL I (2.5 μg/ml; Vector Laboratories). The binding of ECA, PNA, SNA, and MAL I was detected using horseradish peroxidase (HRP)-conjugated streptavidin (Thermo Fisher Scientific) and tetramethylbenzidine substrate (TMB) (BioFX) in an enzyme-linked immunosorbent assay (ELISA) reader (EL-808; BioTek) reading the optical density (OD) at 450 nm. For both the MUNANA assay and the ELLA, the data were fitted by nonlinear regression using Prism 6.05 software (GraphPad). The resulting curves were used to determine the amount of NA protein corresponding to half-maximum lectin binding. The inverse of this amount is a measure of specific activity (activity per amount of protein) and was graphed relative to other NA proteins or substrate-lectin combinations. In a similar way, the specific activity for MUNANA was determined. The mean values of 2 to 4 experiments, with independently generated protein preparations, were graphed. Analysis of the enzymatic specificity of the NA proteins using glycan array analysis was performed as described previously (50). In short, glycan arrays were treated with 20 μg/ml NA protein for 2 h at 37°C, after which the arrays were analyzed for binding with biotinylated ECA (10 μg/ml; Vector Laboratories). Binding of ECA was detected using Alexa Fluor 555-labeled streptavidin (2 μg/ml; Invitrogen). The glycan array values shown are the means and standard errors of 6 glycan spot intensities.

HA and NA binding assays. The binding abilities of HA and N9 proteins were analyzed using fetuin solid-phase binding and hemagglutination assays similarly to what was described previously (40, 51). In brief, 4 μg of purified, soluble trimeric H7 and tetrameric N9 proteins was precomplexed with HRP-conjugated anti-Strep tag mouse antibody (IBA) and with HRP-linked anti-mouse IgG (Dako) in a 4:2:1 molar ratio on ice for half an hour prior to incubation of limiting dilutions on the fetuin-coated (50 μg/ml) or asialofetuin-coated (50 μg/ml; Sigma-Aldrich) 96-well Nunc MaxiSorp plates at 4°C for 2 h. OsC (1 μM; a kind gift from Roche) was added to the N9 protein mixtures in order to inhibit NA enzymatic activity. This concentration is >1,000-fold higher than the OsC 50% inhibitory concentration (IC_{50}) values, which are similar for the different N9 proteins. HA and N9 binding was detected using TMB (BioFX) in an EL-808 ELISA reader (BioTek) reading the OD at 450 nm. The hemagglutination assay was performed as described previously (40). In brief, 2-fold dilutions of the HA or NA antibody complexes described above were incubated with 0.5% chicken erythrocytes for 2 h at 4°C in the presence or absence of 1 μM OsC, with a starting concentration of 40 μg/ml. The glycoprotein binding and hemagglutination assays were performed at least twice in duplicate. The mean values of the results of these experiments were graphed. Binding of the NA proteins to the glycan arrays, containing 135 glycans reported previously (52–54), was

determined similarly to what was described previously for HA proteins (51). N9 proteins (50 μg/ml) were precomplexed with anti-Strep tag mouse antibody (25 μg/ml; IBA) and Alexa Fluor 647-linked anti-mouse IgG (12.5 μg/ml; Invitrogen) similarly to what was described above before their application to the array. The glycan array values shown are the means and standard errors of 6 glycan spot intensities.

Statistical analysis. All statistical analyses were performed by two-tailed *t* test using Prism 6.05 software.

Phylogenetic analysis. All full-length and unique H7 and N9 protein sequences of avian viruses and of the novel H7N9 viruses were downloaded from the GenBank and GISAID databases. H7 and N9 protein trees were constructed by using the PHYLIP neighbor-joining algorithm with the F84 distance matrix. This tree was used as a guide tree to select H7 and N9 sequences representing all main branches of the tree. The selected H7 and N9 proteins were used to construct a summary tree with topology similar to that of the guide tree. The H7 and N9 protein trees were rooted by the A/Anas crecca/Spain/1460/2008 isolate.

SUPPLEMENTAL MATERIAL

Supplemental material for this article may be found at https://doi.org/10.1128/JVI.00049-17.

SUPPLEMENTAL FILE 1, XLS file, 2.6 MB.

ACKNOWLEDGMENTS

We thank Hongbo Guo for stimulating discussions and Roche for kindly providing OsC.

C.A.M.D.H. was supported by the Dutch Ministry of Economic Affairs, Agriculture, and Innovation, Castellum Project "Zoonotic Avian Influenza." M.D. was supported by a grant from the Chinese Scholarship Council, and J.C.P. was supported by a grant from the Kuang Hua Educational Foundation.

The funders had no role in study design, data collection and analysis, decision to publish, or preparation of the manuscript.

REFERENCES

1. Sorrell E, Schrauwen E, Linster M, De Graaf M, Herfst S, Fouchier R. 2011. Predicting 'airborne' influenza viruses: (trans-) mission impossible? Curr Opin Virol 1:635–642. https://doi.org/10.1016/j.coviro.2011.07.003.
2. Shi Y, Zhang W, Wang F, Qi J, Wu Y, Song H, Gao F, Bi Y, Zhang Y, Fan Z, Qin C, Sun H, Liu J, Haywood J, Liu W, Gong W, Wang D, Shu Y, Wang Y, Yan J, Gao GF. 2013. Structures and receptor binding of hemagglutinins from human-infecting H7N9 influenza viruses. Science 342:243–247. https://doi.org/10.1126/science.1242917.
3. Mok CK, Lee HH, Lestra M, Nicholls JM, Chan MC, Sia SF, Zhu H, Poon LL, Guan Y, Peiris JS. 2014. Amino acid substitutions in polymerase basic protein 2 gene contribute to the pathogenicity of the novel A/H7N9 influenza virus in mammalian hosts. J Virol 88:3568–3576. https://doi.org/10.1128/JVI.02740-13.
4. Wu S, Wu F, He J. 2013. Emerging risk of H7N9 influenza in China. Lancet 381:1539–1540. https://doi.org/10.1016/S0140-6736(13)60767-9.
5. Zhou J, Wang D, Gao R, Zhao B, Song J, Qi X, Zhang Y, Shi Y, Yang L, Zhu W. 2013. Biological features of novel avian influenza A (H7N9) virus. Nature 499:500–503. https://doi.org/10.1038/nature12379.
6. Air GM. 2012. Influenza neuraminidase. Influenza Other Respir Viruses 6:245–256. https://doi.org/10.1111/j.1750-2659.2011.00304.x.
7. Colman PM. 1994. Influenza virus neuraminidase: structure, antibodies, and inhibitors. Protein Sci 3:1687–1696. https://doi.org/10.1002/pro.5560031007.
8. Wagner R, Matrosovich M, Klenk H. 2002. Functional balance between haemagglutinin and neuraminidase in influenza virus infections. Rev Med Virol 12:159–166. https://doi.org/10.1002/rmv.352.
9. Krauss S, Webster RG. 2010. Avian influenza virus surveillance and wild birds: past and present. Avian Dis 54:394–398. https://doi.org/10.1637/8703-031609-Review.1.
10. de Graaf M, Fouchier RA. 2014. Role of receptor binding specificity in influenza A virus transmission and pathogenesis. EMBO J 33:823–841. https://doi.org/10.1002/embj.201387442.
11. Watanabe T, Kiso M, Fukuyama S, Nakajima N, Imai M, Yamada S, Murakami S, Yamayoshi S, Iwatsuki-Horimoto K, Sakoda Y. 2013. Characterization of H7N9 influenza A viruses isolated from humans. Nature 501:551–555. https://doi.org/10.1038/nature12392.
12. Zaraket H, Baranovich T, Kaplan BS, Carter R, Song M, Paulson JC, Rehg JE, Bahl J, Crumpton JC, Seiler J. 2015. Mammalian adaptation of influenza A (H7N9) virus is limited by a narrow genetic bottleneck. Nat Commun 6:6553. https://doi.org/10.1038/ncomms7553.
13. Xu R, de Vries RP, Zhu X, Nycholat CM, McBride R, Yu W, Paulson JC, Wilson IA. 2013. Preferential recognition of avian-like receptors in human influenza A H7N9 viruses. Science 342:1230–1235. https://doi.org/10.1126/science.1243761.
14. Ramos I, Krammer F, Hai R, Aguilera D, Bernal-Rubio D, Steel J, García-Sastre A, Fernandez-Sesma A. 2013. H7N9 influenza viruses interact preferentially with α2,3-linked sialic acids and bind weakly to α2,6-linked sialic acids. J Gen Virol 94:2417–2423. https://doi.org/10.1099/vir.0.056184-0.
15. Dortmans J, Dekkers J, Wickramasinghe IA, Verheije M, Rottier P, Van Kuppeveld F, De Vries E, De Haan C. 2013. Adaptation of novel H7N9 influenza A virus to human receptors. Sci Rep 3:3058. https://doi.org/10.1038/srep03058.
16. Xu R, Zhu X, McBride R, Nycholat CM, Yu W, Paulson JC, Wilson IA. 2012. Functional balance of the hemagglutinin and neuraminidase activities accompanies the emergence of the 2009 H1N1 influenza pandemic. J Virol 86:9221–9232. https://doi.org/10.1128/JVI.00697-12.
17. Gambaryan A, Matrosovich M. 2015. What adaptive changes in hemagglutinin and neuraminidase are necessary for emergence of pandemic influenza virus from its avian precursor? Biochemistry 80:872–880. https://doi.org/10.1134/S000629791507007X.
18. Burmeister WP, Ruigrok RW, Cusack S. 1992. The 2.2 A resolution crystal structure of influenza B neuraminidase and its complex with sialic acid. EMBO J 11:49–56.
19. Shtyrya Y, Mochalova L, Bovin N. 2009. Influenza virus neuraminidase: structure and function. Acta Naturae 1:26–32.
20. Kobasa D, Kodihalli S, Luo M, Castrucci MR, Donatelli I, Suzuki Y, Suzuki T, Kawaoka Y. 1999. Amino acid residues contributing to the substrate specificity of the influenza A virus neuraminidase. J Virol 73:6743–6751.
21. Mochalova L, Kurova V, Shtyrya Y, Korchagina E, Gambaryan A, Belyanchikov I, Bovin N. 2007. Oligosaccharide specificity of influenza H1N1 virus neuraminidases. Arch Virol 152:2047–2057. https://doi.org/10.1007/s00705-007-1024-z.
22. Li Y, Cao H, Dao N, Luo Z, Yu H, Chen Y, Xing Z, Baumgarth N, Cardona C, Chen X. 2011. High-throughput neuraminidase substrate specificity

study of human and avian influenza A viruses. Virology 415:12–19. https://doi.org/10.1016/j.virol.2011.03.024.
23. Laver W, Colman P, Webster R, Hinshaw V, Air G. 1984. Influenza virus neuraminidase with hemagglutinin activity. Virology 137:314–323. https://doi.org/10.1016/0042-6822(84)90223-X.
24. Webster RG, Air GM, Metzger DW, Colman PM, Varghese JN, Baker AT, Laver WG. 1987. Antigenic structure and variation in an influenza virus N9 neuraminidase. J Virol 61:2910–2916.
25. Air GM, Laver WG. 1995. Red cells bound to influenza virus N9 neuraminidase are not released by the N9 neuraminidase activity. Virology 211:278–284. https://doi.org/10.1006/viro.1995.1401.
26. Uhlendorff J, Matrosovich T, Klenk H, Matrosovich M. 2009. Functional significance of the hemadsorption activity of influenza virus neuraminidase and its alteration in pandemic viruses. Arch Virol 154:945–957. https://doi.org/10.1007/s00705-009-0393-x.
27. Varghese JN, Colman PM, van Donkelaar A, Blick TJ, Sahasrabudhe A, McKimm-Breschkin JL. 1997. Structural evidence for a second sialic acid binding site in avian influenza virus neuraminidases. Proc Natl Acad Sci U S A 94:11808–11812. https://doi.org/10.1073/pnas.94.22.11808.
28. Lai JC, Garcia J, Dyason JC, Böhm R, Madge PD, Rose FJ, Nicholls JM, Peiris J, Haselhorst T, Von Itzstein M. 2012. A secondary sialic acid binding site on influenza virus neuraminidase: fact or fiction? Angew Chem Int Ed Engl 51:2221–2224. https://doi.org/10.1002/anie.201108245.
29. Kobasa D, Rodgers ME, Wells K, Kawaoka Y. 1997. Neuraminidase hemadsorption activity, conserved in avian influenza A viruses, does not influence viral replication in ducks. J Virol 71:6706–6713.
30. Wang N, Glidden EJ, Murphy SR, Pearse BR, Hebert DN. 2008. The cotranslational maturation program for the type II membrane glycoprotein influenza neuraminidase. J Biol Chem 283:33826–33837. https://doi.org/10.1074/jbc.M806897200.
31. Dai M, Guo H, Dortmans J, Dekkers J, Nordholm J, Daniels R, van Kuppeveld FJ, de Vries E, de Haan CA. 2016. Identification of residues that affect oligomerization and/or enzymatic activity of influenza virus H5N1 neuraminidase proteins. J Virol 90:9457–9470. https://doi.org/10.1128/JVI.01346-16.
32. Zanin M, Duan S, Wong S, Kumar G, Baviskar P, Collin E, Russell C, Barman S, Hause B, Webby R. 2017. An amino acid in the stalk domain of N1 neuraminidase is critical for enzymatic activity. J Virol 91:e00868–16. https://doi.org/10.1128/JVI.00868-16.
33. Baenziger JU, Fiete D. 1979. Structure of the complex oligosaccharides of fetuin. J Biol Chem 254:789–795.
34. Montreuil J. 1975. Complete structure of two carbohydrate units of human serotransferrin. Studies on glycoconjugates XIV. FEBS Lett 50:296–304.
35. von Bonsdorff L, Tölö H, Lindeberg E, Nyman T, Harju A, Parkkinen J. 2001. Development of a pharmaceutical apotransferrin product for iron binding therapy. Biologicals 29:27–37. https://doi.org/10.1006/biol.2001.0273.
36. Wu AM, Wu JH, Tsai M, Yang Z, Sharon N, Herp A. 2007. Differential affinities of Erythrina cristagalli lectin (ECL) toward monosaccharides and polyvalent mammalian structural units. Glycoconj J 24:591–604. https://doi.org/10.1007/s10719-007-9063-y.
37. Sharma V, Srinivas VR, Adhikari P, Vijayan M, Surolia A. 1998. Molecular basis of recognition by Gal/GalNAc specific legume lectins: influence of Glu 129 on the specificity of peanut agglutinin (PNA) towards C2-substituents of galactose. Glycobiology 8:1007–1012. https://doi.org/10.1093/glycob/8.10.1007.
38. Geisler C, Jarvis DL. 2011. Effective glycoanalysis with Maackia amurensis lectins requires a clear understanding of their binding specificities. Glycobiology 21:988–993. https://doi.org/10.1093/glycob/cwr080.
39. Shibuya N, Goldstein IJ, Broekaert WF, Nsimba-Lubaki M, Peeters B, Peumans WJ. 1987. The elderberry (Sambucus nigra L.) bark lectin recognizes the Neu5Ac(alpha 2-6)Gal/GalNAc sequence. J Biol Chem 262:1596–1601.
40. de Vries RP, de Vries E, Bosch BJ, de Groot RJ, Rottier PJ, de Haan CA. 2010. The influenza A virus hemagglutinin glycosylation state affects receptor-binding specificity. Virology 403:17–25. https://doi.org/10.1016/j.virol.2010.03.047.
41. Gao R, Cao B, Hu Y, Feng Z, Wang D, Hu W, Chen J, Jie Z, Qiu H, Xu K. 2013. Human infection with a novel avian-origin influenza A (H7N9) virus. N Engl J Med 368:1888–1897. https://doi.org/10.1056/NEJMoa1304459.
42. Baum LG, Paulson JC. 1991. The N2 neuraminidase of human influenza virus has acquired a substrate specificity complementary to the hemagglutinin receptor specificity. Virology 180:10–15. https://doi.org/10.1016/0042-6822(91)90003-T.
43. Sung JC, Wynsberghe AWV, Amaro RE, Li WW, McCammon JA. 2010. Role of secondary sialic acid binding sites in influenza N1 neuraminidase. J Am Chem Soc 132:2883–2885. https://doi.org/10.1021/ja9073672.
44. Thobhani S, Ember B, Siriwardena A, Boons G. 2003. Multivalency and the mode of action of bacterial sialidases. J Am Chem Soc 125:7154–7155. https://doi.org/10.1021/ja029759w.
45. Langereis MA, Bakkers MJ, Deng L, Padler-Karavani V, Vervoort SJ, Hulswit RJ, van Vliet AL, Gerwig GJ, de Poot SA, Boot W. 2015. Complexity and diversity of the mammalian sialome revealed by nidovirus virolectins. Cell Rep 11:1966–1978. https://doi.org/10.1016/j.celrep.2015.05.044.
46. Bakkers MJ, Zeng Q, Feitsma LJ, Hulswit RJ, Li Z, Westerbeke A, van Kuppeveld FJ, Boons GJ, Langereis MA, Huizinga EG, de Groot RJ. 2016. Coronavirus receptor switch explained from the stereochemistry of protein-carbohydrate interactions and a single mutation. Proc Natl Acad Sci U S A 113:E3111–9. https://doi.org/10.1073/pnas.1519881113.
47. Harbury PB, Zhang T, Kim PS, Alber T. 1993. A switch between two-, three-, and four-stranded coiled coils in GCN4 leucine zipper mutants. Science 262:1401–1407. https://doi.org/10.1126/science.8248779.
48. Stetefeld J, Jenny M, Schulthess T, Landwehr R, Engel J, Kammerer RA. 2000. Crystal structure of a naturally occurring parallel right-handed coiled coil tetramer. Nat Struct Biol 7:772–776. https://doi.org/10.1038/79006.
49. Lambré CR, Terzidis H, Greffard A, Webster RG. 1991. An enzyme-linked lectin assay for sialidase. Clin Chim Act 198:183–193. https://doi.org/10.1016/0009-8981(91)90352-D.
50. Zhu X, McBride R, Nycholat CM, Yu W, Paulson JC, Wilson IA. 2012. Influenza virus neuraminidases with reduced enzymatic activity that avidly bind sialic acid receptors. J Virol 86:13371–13383. https://doi.org/10.1128/JVI.01426-12.
51. de Vries RP, de Vries E, Moore KS, Rigter A, Rottier PJ, de Haan CA. 2011. Only two residues are responsible for the dramatic difference in receptor binding between swine and new pandemic H1 hemagglutinin. J Biol Chem 286:5868–5875. https://doi.org/10.1074/jbc.M110.193557.
52. Wang Z, Chinoy ZS, Ambre SG, Peng W, McBride R, de Vries RP, Glushka J, Paulson JC, Boons GJ. 2013. A general strategy for the chemoenzymatic synthesis of asymmetrically branched N-glycans. Science 341:379–383. https://doi.org/10.1126/science.1236231.
53. Tzarum N, de Vries RP, Zhu X, Yu W, McBride R, Paulson JC, Wilson IA. 2015. Structure and receptor binding of the hemagglutinin from a human H6N1 influenza virus. Cell Host Microbe 17:369–376. https://doi.org/10.1016/j.chom.2015.02.005.
54. Peng W, de Vries RP, Grant OC, Thompson AJ, McBride R, Tsogtbaatar B, Lee PS, Razi N, Wilson IA, Woods RJ, Paulson JC. 2017. Recent H3N2 viruses have evolved specificity for extended, branched human-type receptors, conferring potential for increased avidity. Cell Host Microbe 21:23–34. https://doi.org/10.1016/j.chom.2016.11.004.